Acta Biomaterialia 34 (2016) 30–40

Contents lists available at ScienceDirect

Acta Biomaterialia

journal homepage: www.elsevier.com/locate/actabiomat

Full length article

Extracellular matrix microarrays to study inductive signaling for endoderm specification ☆

D.F. Braga Malta [a,b], N.E. Reticker-Flynn [a], C.L. da Silva [b], J.M.S. Cabral [b], H.E. Fleming [a], K.S. Zaret [c], S.N. Bhatia [a,d,f,g,1], G.H. Underhill [e,*,1]

[a] Massachusetts Institute of Technology, Cambridge, MA, United States
[b] Department of Bioengineering and IBB-Institute for Bioengineering and Biosciences, Instituto Superior Técnico, Universidade de Lisboa, Portugal
[c] University of Pennsylvania, Philadelphia, PA, United States
[d] The Howard Hughes Medical Institute, Cambridge, MA, United States
[e] University of Illinois at Urbana-Champaign, Urbana, IL, United States
[f] Koch Institute for Integrative Cancer Research, Massachusetts Institute of Technology, Cambridge, MA 021392, United States
[g] Institute for Medical Engineering & Science, Massachusetts Institute of Technology, Cambridge, MA 02139, United States

ARTICLE INFO

Article history:
Received 11 September 2015
Received in revised form 29 January 2016
Accepted 10 February 2016
Available online 12 February 2016

Keywords:
High-throughput
Microarray
Extracellular matrix
Liver
Pancreas

ABSTRACT

During tissue development, stem and progenitor cells are faced with fate decisions coordinated by microenvironmental cues. Although insights have been gained from *in vitro* and *in vivo* studies, the role of the microenvironment remains poorly understood due to the inability to systematically explore combinations of stimuli at a large scale. To overcome such restrictions, we implemented an extracellular matrix (ECM) array platform that facilitates the study of 741 distinct combinations of 38 different ECM components in a systematic, unbiased and high-throughput manner. Using embryonic stem cells as a model system, we derived definitive endoderm progenitors and applied them to the array platform to study the influence of ECM, including the interactions of ECM with growth factor signaling, on the specification of definitive endoderm cells towards the liver and pancreas fates. We identified ECM combinations that influence endoderm fate decisions towards these lineages, and demonstrated the utility of this platform for studying ECM-mediated modifications to signal activation during liver specification. In particular, defined combinations of fibronectin and laminin isoforms, as well as combinations of distinct collagen subtypes, were shown to influence SMAD pathway activation and the degree of hepatic differentiation. Overall, our systematic high-throughput approach suggests that ECM components of the microenvironment have modulatory effects on endoderm differentiation, including effects on lineage fate choice and cell adhesion and survival during the differentiation process. This platform represents a robust tool for analyzing effects of ECM composition towards the continued improvement of stem cell differentiation protocols and further elucidation of tissue development processes.

Statement of Significance

Cellular microarrays can provide the capability to perform high-throughput investigations into the role of microenvironmental signals in a variety of cell functions. This study demonstrates the utility of a high-throughput cellular microarray approach for analyzing the effects of extracellular matrix (ECM) in liver and pancreas differentiation of endoderm progenitor cells. Despite an appreciation that ECM is likely involved in these processes, the influence of ECM, particularly combinations of matrix proteins, had not been systematically explored. In addition to the identification of relevant ECM compositions, this study illustrates the capability of the cellular microarray platform to be integrated with a diverse range of cell fate measurements, which could be broadly applied towards the investigation of cell fate regulation in other tissue development and disease contexts.

☆ Part of the High Throughput Approaches to Screening Biomaterials Special Issue, edited by Kristopher Kilian and Prabhas Moghe.

* Corresponding author.
E-mail address: gunderhi@illinois.edu (G.H. Underhill).

[1] Indicates co-senior authors.

http://dx.doi.org/10.1016/j.actbio.2016.02.014
1742-7061/

1. Introduction

To harness the potential of stem and progenitor cells for cell replacement therapies as well as drug discovery and disease modeling platforms, a more complete understanding of the role of microenvironmental signals in cell fate specification is required. Efforts at the interface of bioengineering and cell biology have sought to develop improved culture models which recapitulate *in vivo* microenvironments in order to study cell differentiation and tissue development. These approaches have emphasized the reduction of multicomponent cellular microenvironments into distinct individual signals that can be tightly controlled in engineering environments, and have provided insights into regulatory mechanisms. However, the understanding of how combinations of microenvironmental cues act together to regulate stem cell fates has been restricted by the iterative nature of these methods. Cellular microarrays can facilitate the combination of distinct biochemical cues in a high-throughput manner, and the quantitative assessment of how such combinatorial microenvironments regulate cell fate decisions. Cellular microarray platforms have been employed to study neural stem cell fate [1], and towards the clarification of the role of the microenvironment in the mammary gland [2]. Anderson and co-workers used this approach to identify synthetic materials that maintain human embryonic stem cell pluripotency [3]. We have previously developed an extracellular matrix (ECM) microarray, which has been applied towards the examination of hepatocyte survival and stem cell differentiation [4]. Recently, we expanded the throughput of this platform towards the study of lung adenocarcinoma cell adhesion and potential mechanisms underlying metastasis [5]. Here, we have employed an ECM microarray-based approach towards the systematic analysis of liver and pancreas differentiation of endoderm progenitor cells within distinct ECM microenvironments.

In vivo, ventral foregut endoderm is differentially patterned to form liver and pancreas by signals from adjacent mesodermal tissues. In particular, liver specification has been demonstrated to require cooperative signaling induced by fibroblast growth factors (FGFs) secreted by cardiac mesoderm and bone morphogenetic protein (BMP)-4 secreted by the septum transversum mesenchyme [6–8]. In contrast, ventral endoderm cells which are spatially separated from these signals initiate pancreatic differentiation. Pancreatic fate, revealed by studies in chick and zebrafish, is a result of retinoic acid (RA) [9], BMP [10] and hedgehog [11,12] signaling. FGF10 was also shown to be important in the maintenance of Pdx1-positive pancreatic cells *in vivo* [13,14]. Together with growth factor signaling, epigenetic changes have additionally been demonstrated to be critical for directing the fate of endoderm cells, for example, increased methylation of distinct promoter regions has been identified to be necessary for hepatic (liver)-lineage commitment [15]. Notably, limited studies have examined the expression of ECM components during liver [16,17] and pancreas [18] development, or during the *in vitro* differentiation of stem and progenitor cells [19–21]. Thus, the role of ECM in the differentiation of hepatic and pancreatic lineages remains primarily unclear.

In this report, we demonstrate an unbiased high-throughput approach for identifying ECM combinations that modulate liver and pancreas differentiation and for investigating the signaling events underlying cell lineage commitment. In particular, we illustrate the scope of this approach by employing multiple iterations of an ECM microarray platform consisting of 741 unique pairwise combinations of 38 ECM molecules, as well as subsequent arrays formulated from focused subsets of ECM combinations for defined mechanistic studies. Overall, our studies highlight the capabilities of a high-throughput cell microarray platform for deconstructing the complex signals regulating endoderm differentiation.

2. Materials and methods

2.1. ECM array fabrication and cell seeding

Vantage acrylic slides (CEL-1 Associates VACR-25C) were coated with polyacrylamide gel pads (60 × 22 mm) as described previously [22]. ECM domains were arrayed using a DNA Microarray spotter (Cartesian Technologies Pixsys Microarray Spotter and ArrayIt 946 Pins) from 384-well V-bottom source plates containing the ECM combinations previously prepared using a Tecan EVO 150 liquid handler. Specifically, 10 μl volumes of ECM combinations were prepared in the 384-well source plate using the liquid handler, and these ECM combinations were prepared to a final concentration of 200 μg/ml in a previously described buffer [4], consisting of 100 mM acetate, 5 mM EDTA, 20% glycerol, 0.25% Triton X-100, and pH adjusted to 5.0. 741 combinations were spotted in replicates of five and rhodamine dextran (Invitrogen) was arrayed to dually serve as a negative control for cell adhesion and as an alignment reference for imaging analysis. ECM arrays were stored in a humidified chamber at 4 °C, until later use. The following ECM molecules were incorporated into the 741 combination array: Collagen I, Collagen II, Collagen III, Collagen IV, Fibronectin, Laminin, Chondroitin Sulfate, Merosin (Millipore), Collagen V, Collagen VI (BD Biosciences), Aggrecan, Elastin, Keratin, Mucin, Heparan Sulfate, Superfibronectin, Fibrin, Hyaluronan (Sigma), Tenascin-R, F-Spondin, Nidogen-2, Biglycan, Decorin, Galectin 1, Galectin 3, Galectin 4, Galectin 8, Thrombospondin-4, Osteopontin, Osteonectin, Testican 1, Testican 2, Tenascin-C, Nidogen-1, Vitronectin, Rat, Agrin, Brevican (R&D Systems) and Galectin 3c (EMD Biosciences).

Prior to cell seeding, slides containing arrayed ECM domains were washed in PBS and treated with UV light to reduce potential contamination. Slides were placed in a specialized seeding device that holds the top surface of the slides flush with the bottom of the well. Three million cells were seeded on each slide in 5 mL of media and incubated for 12 h at 37 °C. After cell attachment, slides were transferred to quadriperm plates (NUNC, 167063), and fresh media was added. For differentiation experiments, arrays containing adherent cells were cultured for 72 h in defined soluble induction conditions (described below) and medium with induction factors was changed daily.

2.2. Microarray immunostaining and analysis

At various time points of differentiation induction, slides were washed (three times with PBS) and fixed with 4% paraformaldehyde. Slides were then treated with 0.1% Triton-X in PBS, which also contained Hoechst (Invitrogen) for labeling cell nuclei. Following an additional wash with PBS, slides were stored for 1 h in a blocking solution containing the animal serum corresponding to the secondary antibody. Slides were then incubated with primary antibodies against AFP and Pdx1 (Millipore) overnight at 4 °C. Secondary antibody (Invitrogen) incubation for 45 min followed after PBS washes. Slides were finally washed and mounted with Fluoromount-G (Southern Biotech) and stored at 4 °C until imaging. The entire slide was imaged using a Nikon Ti-Eclipse inverted fluorescence microscope and NIS Elements Software (Nikon). Image processing and analysis was performed in MATLAB (Mathworks) and nuclei and marker intensity quantification using CellProfiler [23]. Replicate spots ($\geqslant$5 per slide) on each slide were averaged and those whose values were greater than one standard deviation above or below the mean of the replicates were excluded. Slides were normalized to the mean of their non-zero adhesion (cell nuclei #) or protein immunostaining values, to allow for comparison across independent experiments.

2.3. mESC culture and differentiation

Sox17/GFP reporter mouse embryonic stem cells [24,25] were maintained in a feeder dependent culture on mitotically inactivated (Mitomycin C) mouse embryonic fibroblast in media (DMEM F12 medium supplemented with 15% knockout serum replacement, non-essential amino acids, glutamine, penicillin/streptomycin) supplemented with LIF (Millipore). For differentiation towards endoderm, cells were trypsinized and plated on gelatin (sigma) coated 10 cm culture plates and cultured for 7 days in low serum differentiation medium, which consisted of Advanced RPMI 1640 (Invitrogen) base media supplemented with 2% FBS, and further contained 2 μM IDE-2 (Stemgent). The following conditions were used for hepatic and pancreatic induction within the array: hepatic-low serum differentiation medium plus BMP4 (50 ng/ml R&D Systems) and bFGF (10 ng/ml R&D Systems); pancreatic-low serum differentiation medium plus c-KAAD (0.75 μg/ml EMD Bioscience), FGF10 (50 ng/ml R&D Systems) and retinoic acid (2 μg/ml Sigma). For off-array hepatic differentiation, cells in 10 cm culture plates following IDE-2 treatment and endoderm differentiation, were further cultured for 3 days in low serum differentiation medium containing 50 ng/ml BMP4 and 10 ng/ml bFGF.

2.4. Flow activated cell sorting

Definitive endoderm cells were enriched prior to array seeding using FACS, selecting for cells that were sox17-positive (GFP-positive) and CD26-negative. Briefly, cells were harvested following IDE-2 treatment, dispersed to a single cell population, incubated with rat anti-CD26 (FITC, BD Biosciences) at 4 °C for 20 min, washed three times with PBS containing 1% FBS, and then incubated with APC-labeled anti-rat secondary antibody. For enrichment of Liv2-positive hepatic cells, cells were sequentially incubated with rat anti-Liv2 (MBL International) and APC-labeled anti-rat secondary antibodies. Cells were collected with a MoFlo cell sorter (Beckman Coulter).

2.5. Mouse embryo preparation and immunofluorescent staining

Whole mount immunostaining was performed as described [26,27]. Rat monoclonal antibody to Merosin (laminin α2) was purchased from Abcam and used at 1:100 dilution. Alexa Fluor secondary antibody was used at 1:500 dilution. Specimens were counterstained with DAPI for visualization of cell nuclei. Whole mount immunostained embryos were fixed in 4% paraformaldehyde, dehydrated in 30% sucrose in PBS and embedded in OCT compound for cryosectioning. Experiments using animals were in compliance with institutional ethical use protocols.

2.6. Statistical analyses

Unless otherwise specified, data presented as mean ± S.E.M. A minimum of three independent experiments were performed for each study. Student's *t*-tests were performed utilizing Minitab software comparing the groups of interest using options denoting a two-tailed, two-sample comparison with unequal variance. Clustering analysis was performed based on Euclidean distances using Spotfire (Tibco) with the hierarchical clustering algorithm. For large-scale array experiments, one-way ANOVA with Tukey's Multiple Comparison Test was used to analyze statistical significance.

3. Results

3.1. Microarray-based analysis of endoderm cell adhesion and differentiation

To investigate cell-ECM interactions during liver and pancreatic commitment, we fabricated microarrays consisting of 4000 individual (150 micrometer) domains ('spots') presenting one of 741 different ECM microenvironments (or non-adhesive and collagen I-only controls) that appear in quintuplicate on a single microscope slide. The total concentration of ECM within each spotted domain was held constant at 200 μg/ml. The composition of the 741 unique spots are the result of all single and pairwise combinations of 38 commercially available ECM molecules (Table 1), which represent a complex library of environments suitable for the study of the influence of ECM on endoderm cell differentiation.

Following fabrication, we seeded the arrays with definitive endoderm (DE) cells, and adapted our previously established analysis pipeline [5], to quantify adhered cell numbers, differentiation marker expression, and signaling pathway activity within the unique ECM environments over time (Fig. 1A). DE cells were obtained through the differentiation and fluorescence activated cell sorting (FACS)-based enrichment of mouse embryonic stem (ES) cells. Specifically, mouse ES cells expressing a GFP reporter for Sox17, an endoderm marker, were cultured for 7 days in the presence of a small molecule inducer of endoderm differentiation, IDE-2 [28]. Prior to seeding the arrays, DE cells were enriched from the mixed population of differentiated cells by FACS, selecting for cells that were positive for Sox17/GFP but that did not express CD26, a known visceral endoderm marker. Approximately 40% of day 7 differentiated cells were Sox17+/CD26− (representative experiment illustrated in Supplemental Fig. 1A), and consistent with the removal of visceral endoderm cells, the sorting process reduced the expression of a panel of visceral endoderm genes (Supplemental Fig. 1B). The sorted cells were seeded on the ECM array (3×10^6 cells per slide) overnight in endoderm differentiation medium to establish the DE ECM array platform (Fig. 1B). This cell density and seeding time were optimized such that near confluent islands of DE cells were obtained on many of the ECM combinations. Specifically, the DE cells were capable of robust adhesion to distinct ECM combinations, as illustrated by the reproducibility between replicate spots in the array (Fig. 1C). Further, visualization of the average adhesion to each domain, through the staining and quantification of cell nuclei per spot, allowed for the identification of ECM combinations that most effectively support adhesion of DE cells (red squares, Fig. 1D). Among the conditions that most effectively supported DE cell adhesion, combinations containing either fibronectin or laminin (α1) were highly represented.

To assess the initial differentiation status of the seeded DE population shortly after adherence to the ECM array, we evaluated the

Table 1
ECM molecules presented in the ECM array. ECM array comprises 4000 addressable features per array that are the result of all single and pairwise combinations of the ECM molecules present in this table to a total of 741 unique ECM environments that are represented in quintuplicate plus positive (Collagen I) and negative (dextran, no ECM) controls.

Collagen I (CI)	Tenascin-C (Ten-C)	Nidogen-1 (Nid-1)
Collagen II (CII)	Tenascin-R (Ten-R)	Nidogen-2 (Nid-2)
Collagen III (CIII)	Chondroitin Sulfate (Chon)	Heparan Sulfate (HepSul)
Collagen IV (CIV)	Aggrecan (Agg)	Hyaluronic Acid (Hya)
Collagen V (CV)	Decorin (Dec)	Biglycan (Bigly)
Collagen VI (CVI)	Elastin (Elas)	Galectin 1 (Gal-1)
Fibronectin (Fib)	Keratin (Ker)	Galectin 3 (Gal-3)
Laminin (α1) (Lam)	Mucin (Muc)	Galectin 3c (Gal-3c)
Merosin (laminin α2) (Mer)	Agrin (Agr)	Galectin 4 (Gal-4)
Vitronectin (Vit)	F-Spondin (F-Spo)	Fibrin (Fibrin)
Galectin 8 (Gal-8)	Testican 1/SPOCK1 (Test-1)	Testican 2/SPOCK2 (Test-2)
Osteopontin (Osteo)	SPARC/Osteonectin (SPARC)	Thrombospondin-4 (Thom-4)
Brevican (Bre)	Superfibronectin (SupFib)	

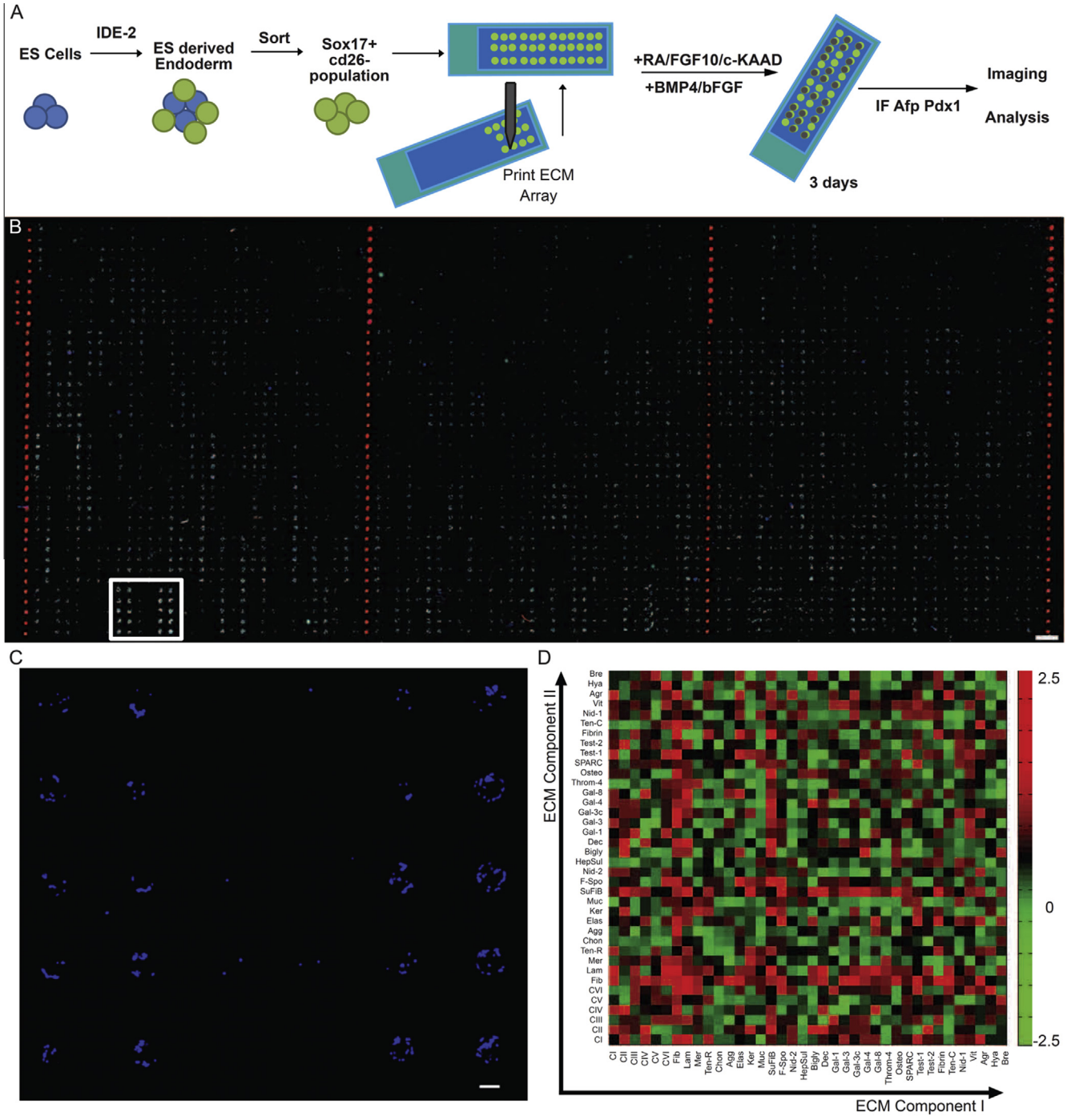

Fig. 1. Extracellular matrix microarray-based approach for investigating endoderm cell function and differentiation. (A) Schematic of experimental approach. ECM microarrays are comprised of all single and pairwise combinations of 38 ECM molecules presented in quintuplicate to form a total of 4000 features (including positive and negative controls) on a single microscope slide. ECM arrays are prepared by contact spotting of ECM molecule combinations on a polyacrylamide hydrogel that was previously formed on the slide surface. Mouse ES are differentiated to the endoderm stage and selected via flow cytometry-based sorting for definitive endoderm characteristic markers (sox17+ and CD26−) prior to seeding on the ECM arrays. Arrays are treated with cocktails of soluble factors to induce hepatic (BMP4/bFGF) or pancreatic (RA/FGF10/c-KAAD) differentiation and at specific time points slides are fixed, stained (immunofluorescence, IF) for specific cell markers, followed by imaging of the entire slide. Acquired images are processed in Matlab and CellProfiler [5,44], and each ECM condition is quantitatively evaluated for cell number and specific marker expression. (B) Representative image of complete ECM microarray 12 h post-seeding with definitive endoderm cells. Image represents the 4000 features in the array, and cell nuclei and cytoplasm are labeled with fluorescent dyes. Red features are rhodamine-dextran spots utilized as negative controls and for alignment of image acquisition. Scale bar = 1 mm. (C) Inset from panel B, including cell nuclei label only and illustrating a representative set of ECM islands in quintuplicate. Scale bar = 100 μm. (D) Heatmap quantification of endoderm cell adhesion 12 h post-seeding. Each feature represents the combination formed by 2 different ECM molecules on the *x* and *y* axes, and color code represents cell nuclei intensity, which is a surrogate measure of cell number per ECM domain. Data is normalized to allow comparison between biological replicates. 0 represents the average of the slide and positive and negative values indicate the number of standard deviations from the mean.

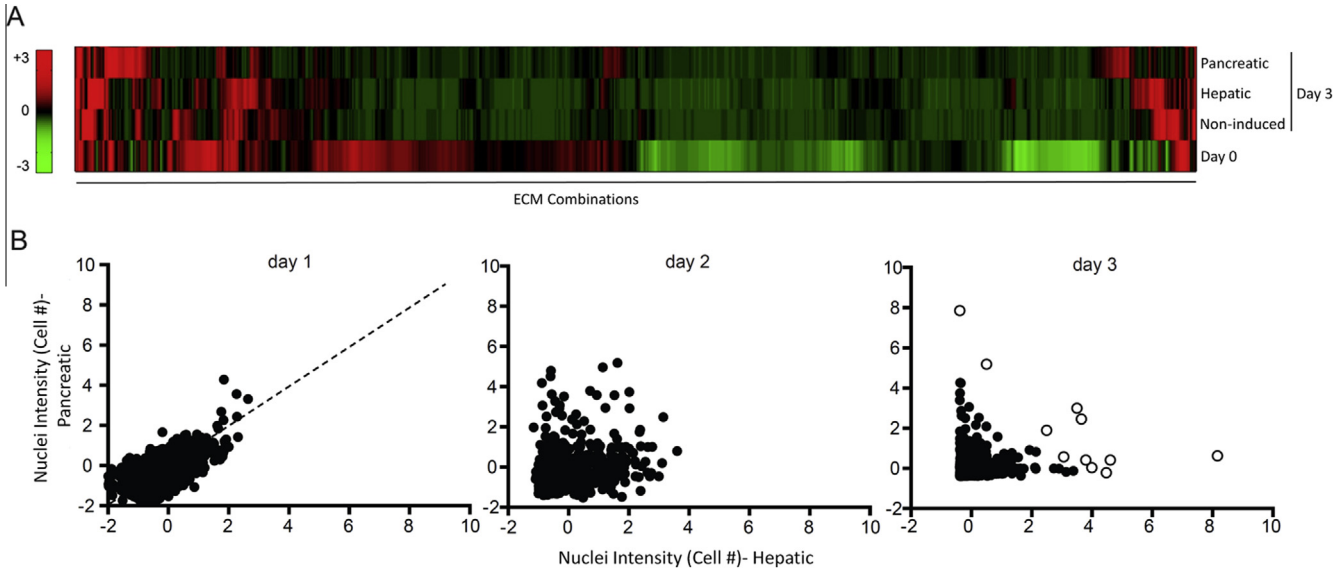

Fig. 2. Quantification of cell numbers within ECM array following induction of hepatic and pancreatic differentiation. (A) Heatmap comparison of cell numbers for each ECM combination for Day 0 (post-12 h seeding of definitive endoderm) and following 3 day treatment with hepatic (BMP4/bFGF), pancreatic (RA/FGF10/c-KAAD), or non-induced (basal differentiation medium only). Data are normalized and color scale indicates standard deviations from the mean. (B) Scatter plot representations of the evolving cell number profiles. Each circle represents a single ECM condition, for which the nuclei intensity (cell number) in hepatic-inducing conditions is plotted versus nuclei intensity (cell number) in pancreatic-inducing conditions. With increasing time of differentiation, an increasing number of ECM conditions diverge from the $y = x$ line and align closer to the axes. ECM conditions indicated by white circles are statistically significant ($p < 0.05$) (one-way ANOVA) compared to the overall mean.

expression of DE markers Sox17 and Foxa2 by immunofluorescence (Supplemental Fig. 2). Twelve hours post-seeding, cells adherent on the ECM array maintained expression of Sox17 and Foxa2 (Supplemental Fig. 2B–C). Thus, for subsequent experiments investigating the effects of ECM on liver and pancreas specification, the 12 h post-seeding time point represents day 0 of the array differentiation protocols.

3.2. Assessment of ECM adhesion profiles upon induction of hepatic and pancreatic differentiation of endoderm

Hepatic and pancreatic specification of DE cells is regulated *in vivo* by adjacent tissues that secrete growth and morphogenic factors. By employing the large-scale ECM array, we investigated potential interactions between ECM compositions and known soluble cues that induce hepatic or pancreatic differentiation of endoderm progenitor cells. Following adhesion of DE cells onto the ECM arrays, we treated replicate arrays with hepatic-inducing (+BMP4/bFGF) or pancreatic-inducing (+RA/c-KAAD/FGF10) soluble conditions for 3 days, and quantified the cell number bound to each ECM domain, based on the intensity of nuclei stain per spot, to generate cell adhesion/survival profiles of the differentiating cells. A comparison of these profiles is illustrated in Fig. 2A, which includes the normalized cell number distributions across the 741 ECM combinations for DE prior to soluble induction (Day 0), as well as following hepatic/pancreatic induction and a non-induced control condition at Day 3. This heat map quantification demonstrates that there are numerous ECM combinations, approximately 180 (24%) conditions, that support the adhesion of mouse DE cells prior to differentiation induction, but lose this supportive capacity during differentiation and/or continued cell culture. In addition, treatment with either hepatic or pancreatic inducing factors leads to distinct adhesion profiles of differentiating cells.

To further explore the kinetic evolution of these distinct profiles, we performed the same experiment, and quantified the adherent cell numbers every 24 h (day 1, day 2, and day 3) after the addition of either hepatic-inducing or pancreatic-inducing soluble factors. At the first time point, the number of adherent cells observed in each differentiation condition align in the $x = y$ axis when plotted relative to each other, indicating no overt ECM-mediated selection for or against cell binding or division when in the presence of growth factors that promote either hepatic or pancreatic fate (Fig. 2B). However, with increased time of exposure to the differentiation conditions, the specific ECM environment to which the cells are adhered appears to influence the bound cell number. Specifically, the number of cells adhered to given ECM combinations aligns more closely with the vertical (pancreatic) or horizontal (hepatic) axis after 48 and 72 h, suggesting that distinct effects of hepatic and pancreatic conditions arise based on ECM context. These results suggest that the differentiation of DE cells may be accompanied by changes in the expression/functionality of adhesion receptors and/or a reduction in pro-survival signals that fail to support differentiating cells in the presence of certain ECM combinations.

In order to explore the possibility that ECM conditions could provide differential survival signals influencing the degree of apoptosis, we performed immunostaining and quantified the levels of activated (cleaved) caspase-3 at multiple time points during differentiation. We observed that the composition of the ECM environment can influence the degree of caspase-3 activation (Supplemental Fig. 3). Furthermore, these data illustrate that for specific ECM combinations, hepatic and pancreatic inducing conditions can lead to differential activation of caspase-3 (Supplemental Fig. 3).

3.3. Evaluation of ECM effects on hepatic and pancreatic lineage differentiation

In addition to total bound cell number, we next sought to examine the influence of ECM binding on the degree of differentiation towards hepatic or pancreatic lineages. Within the large-scale (741 combinations) ECM microarray, we performed immunostaining to detect the expression of alpha-fetoprotein (AFP), a hepatic lineage marker, and Pdx1, a pancreatic lineage marker, 72 h after hepatic or pancreatic differentiation induction,

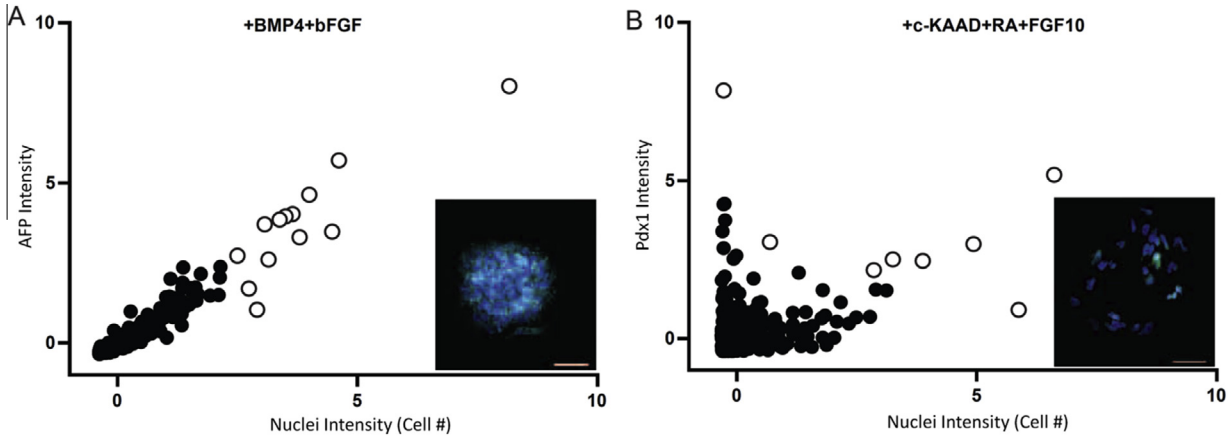

Fig. 3. Quantification of hepatic and pancreatic differentiation markers. (A) Following 3 day treatment of ECM microarrays containing definitive endoderm cells with hepatic (BMP4/bFGF) inducing conditions, expression of the hepatic marker alpha-fetoprotein (AFP) and cell number was quantitatively measured. Each circle represents a distinct ECM condition, for which the AFP intensity per ECM domain is plotted versus nuclei intensity (cell number). (B) Scatter plot of pancreatic marker (Pdx1) intensity per ECM domain plotted versus nuclei intensity (cell number), following 3 day treatment of endoderm with pancreatic (RA/FGF10/c-KAAD) inducing conditions. White circles indicate ECM combinations that are statistically significant ($p < 0.05$) (one-way ANOVA) compared to the mean for either marker intensity of nuclei intensity. Insets are representative ECM domains immunostained for nuclei and AFP or Pdx1, respectively. Scale bars = 50 μm.

Table 2
31 ECM combinations included in subset-focused ECM array.

Fib + Mer	Vit + Gal-1	CII + Gal-1	CIV
Fib	Vit + Nid-1	CII + Agr	CI
Mer	Gal-3 + Vit	CII + Bigly	CI + CIV
Fib + Agg	Throm-4 + Vit	CII	CI + Nid-1
Fib + Elas	Bigly + Vit	CII + CIV	CI + Dec
Lam + SupFib	Vit	CIV + Fib	SPARC + Fibrin
Lam	CII + SupFib	CIV + Vit	Gal-3 + Ten-C
SupFib	CII + Test-1	CVI + SPARC	

respectively. We quantified the intensity of signal per spot derived from both cell number (nuclei) and the expression of differentiation markers (AFP or Pdx1) and analyzed the intersection profiles to correlate cell number with degree of differentiation.

Upon hepatic differentiation (Fig. 3A), we observed a strong correlation between cell number and amount of AFP expression. Specifically, ECM combinations aligned in the $x = y$ axis of the AFP versus nuclei scatter plot, demonstrating that per ECM domain, an elevation in the signal intensity that represents the number of bound cells corresponded with increased AFP expression (Fig. 3A). The introduction of pancreatic promoting factors resulted in a different profile (Fig. 3B). In this case, only a subset of ECM combinations demonstrated a positive correlation between cell number and Pdx1 expression, as was observed for the majority of conditions during hepatic differentiation. In contrast, several other combinations aligned closer to the horizontal or the vertical axis, indicating that for pancreatic specification, the role of ECM in supporting cell number is less correlated with the effects of ECM on Pdx1 expression.

To further probe the effects of ECM combinations, we utilized the data from the large-scale array to select 31 ECM conditions of particular interest, and performed differentiation studies using focused arrays containing these ECM compositions (Table 2). These specific ECM conditions included any combination of two ECM proteins which exhibited a statistically significant effect on hepatic or pancreatic differentiation (Fig. 3), as well as the individual ECM components present within these select combinations. Among the conditions included in this focused array were the combinations fibronectin + merosin, laminin + superfibronectin, and combinations of collagens I, II, and IV (Fig. 4A–C). Notably, for these conditions, the combination of two distinct molecules yields effects that were distinct from those observed in the presence of the same ECM molecules presented in isolation. For example, fibronectin alone induced moderate differentiation and supported significant adhesion (cell numbers), while the presence of only merosin supported neither differentiation nor an increase in cell number. However, when combined, differentiation based on AFP expression was enhanced (Fig. 4A). Combining laminin with superfibronectin yields a similar outcome, in that both hepatic differentiation and total cell number were enhanced relative to DE cells cultured in the presence of either ECM in isolation (Fig. 4A). The analysis of the combinations of CI, CII and CIV also revealed outcomes that would not have been predicted based on the results observed in single-ECM niches. Specifically, none of the individual molecules supported substantial cell numbers, but the combination of CIV with either CI or CII improved the maintenance of cell number (Fig. 4B). Regarding differentiation induction, AFP expression was promoted by either CII or CIV both alone and in combination, but CI and CIV only supported hepatic differentiation when combined (Fig. 4B).

Additional results from the focused 31 ECM array studies are illustrated in Supplemental Fig. 4, which includes the hepatic differentiation data for conditions not highlighted in Fig. 4, as well as the complete 31 ECM condition panel data for pancreatic (Pdx1 expression) differentiation. Overall, when comparing the ECM conditions that best supported hepatic and pancreatic differentiation, we noted that two combinations (fibronectin + merosin (laminin α2) and laminin (α1) + superfibronectin) are among the most robust domains for both hepatic and pancreatic differentiation. Additionally, other ECM combinations selectively supported hepatic or pancreatic differentiation. For example, hepatic, but not pancreatic, differentiation was robust in the presence of fibronectin + aggrecan, fibronectin + elastin, collagen II + galectin1, or collagen II + biglycan. In contrast, pancreatic differentiation was selectively supported by collagen IV + fibronectin (Supplemental Fig. 4). We further examined mRNA expression of AFP and Pdx1 genes following either hepatic or pancreatic differentiation within a multiwell plate format, in which well surfaces were treated with the combination of ECM proteins fibronectin and merosin prior to cell seeding (Supplemental Fig. 5). These data confirm that the most pronounced AFP and Pdx1 expression levels are observed following hepatic and pancreatic induction, respectively.

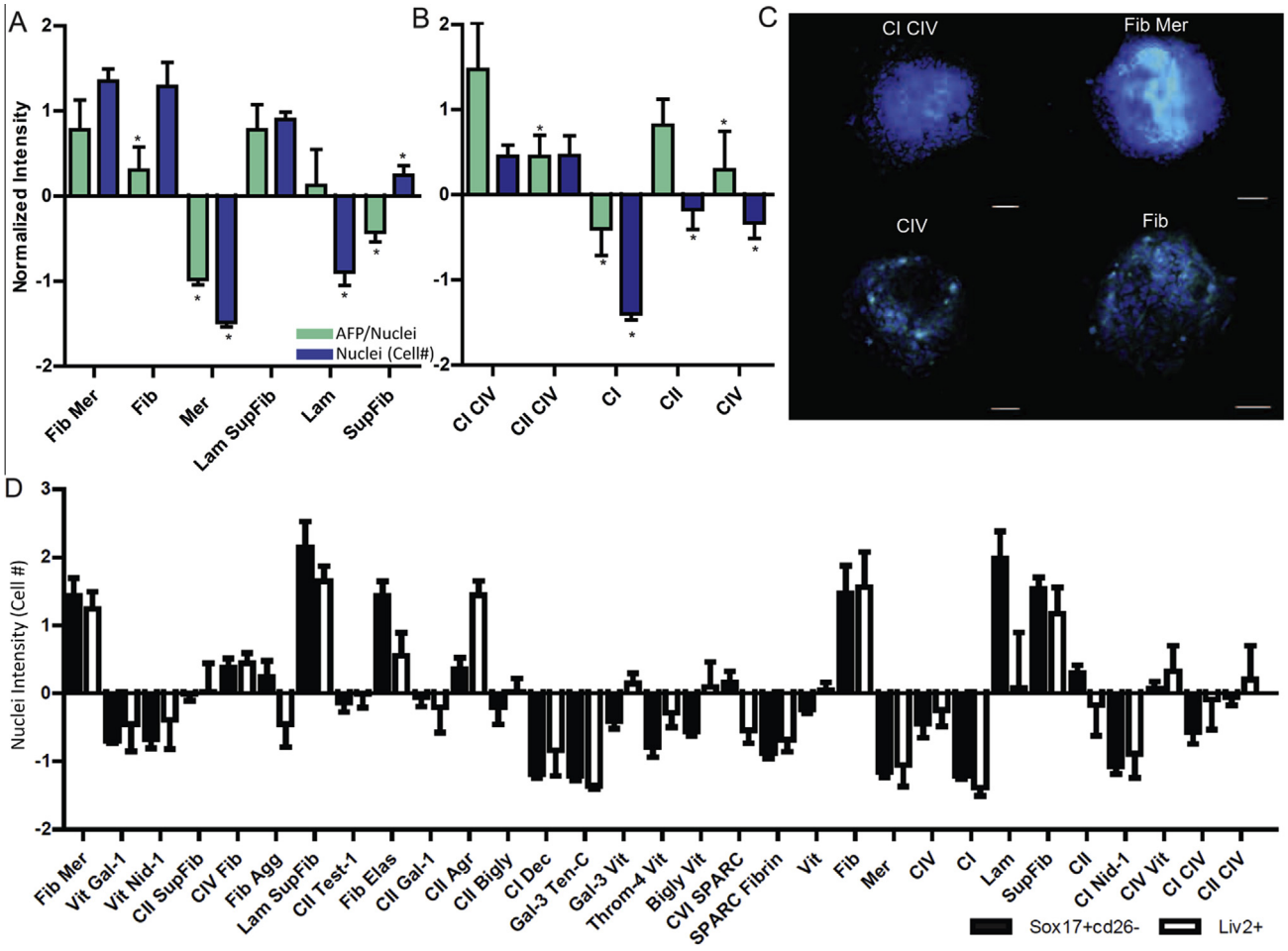

Fig. 4. Distinct effects of ECM combinations during hepatic specification of endoderm. (A–C) Focused ECM microarrays consisting of a subset of 31 ECM conditions were fabricated and utilized for the comparison of select ECM combinations and single ECM components of these combinations. (A) Nuclei intensity (cell number) (blue bars) and AFP intensity normalized by nuclei intensity (green bars) are illustrated for the combinations fibronectin + merosin and laminin + superfibronectin, as well as the single ECM components of these combinations. * = $p < 0.05$, compared to fibronectin + merosin condition. (B) Select combinations and single components of collagen I, collagen II, and collagen IV. * = $p < 0.05$ (Student's *t*-test), compared to collagen I + collagen IV condition. (C) Representative ECM islands at day 3 post-induction towards hepatic lineage. Scale bars = 50 μm. (D) Direct comparison of cell numbers adherent to ECM combinations following differentiation of Sox17+/CD26− endoderm cells within the array (black bars) versus Liv2+ hepatic cells differentiated 'off-array' and subsequently seeded on ECM arrays (white bars).

3.4. Comparison to standard multi-well plate culture

To confirm that the process of hepatic differentiation that occurred while bound to the arrays was similar to differentiation that takes place in standard multi-well plates, we utilized the 31-combination focused arrays to evaluate whether cells that underwent array differentiation or 'off-array' differentiation exhibited alterations in their ECM adherence profiles. Specifically, we seeded 31 ECM arrays with ES cell-derived DE cells and cultured these arrays in hepatic-promoting conditions for 3 days (as in Fig. 4A–B). We directly compared the number of adherent cells per ECM condition to the adhesion pattern of Liv2-expressing hepatic cells, which were seeded on the array for 12 h after 3 days of differentiation in standard culture plates and FACS-based enrichment. Notably, the cell number profiles of these independent conditions exhibit a strong correlation, with only a few select conditions exhibiting any difference between D3 array-differentiated DE cells and 'off-array' differentiated Liv2 + cells (Fig. 4D). These results suggest that for the subset of ECM combinations examined here, the array culture format does not significantly influence the profile of ECM-based adhesion.

3.5. Examination of merosin expression in vivo

Merosin preparations collectively consist of multiple laminin isoforms sharing the α2 chain, and deficiencies in laminin α2 have been associated with congenital muscular dystrophies [29]. A role for merosin/laminin α2 in the differentiation of endoderm lineage differentiation has not previously been identified. Immunostaining for merosin in day E8.5 mouse embryos demonstrated expression of merosin in the area of the foregut endoderm, as well as in the ventral endoderm and yolk sac (Fig. 5), suggesting that merosin, together with localized secreted factors and potentially other ECM components may play a role in endoderm differentiation at this stage.

3.6. Application of the ECM microarray platform towards systematic analysis of signaling mechanisms

In addition to performing a quantitative assessment of protein expression to track phenotypic differentiation, we also utilized the microarray platform to investigate signaling pathway activation patterns that may underlie the observed ECM effects. We

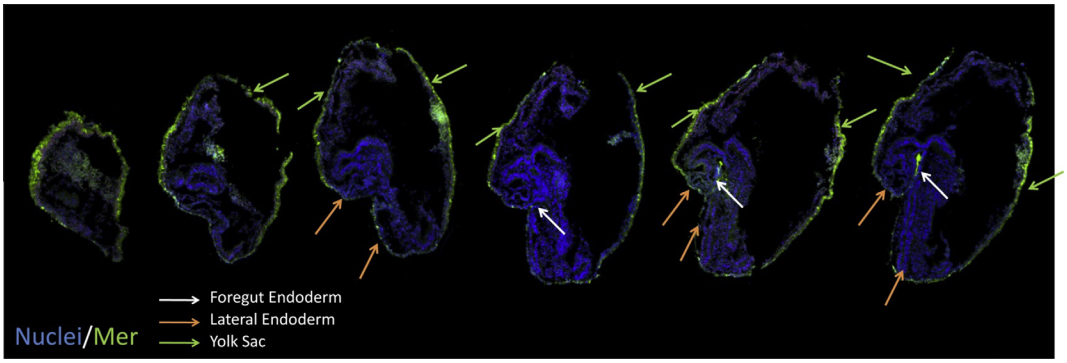

Fig. 5. Expression of merosin in mouse embryo sections. Immunofluorescent staining of merosin (green) and cell nuclei (blue) in mouse embryo sections at embryonic day 8.5. Merosin expression is observed in foregut endoderm, lateral endoderm, and yolk sac. Multiple adjacent sections are shown.

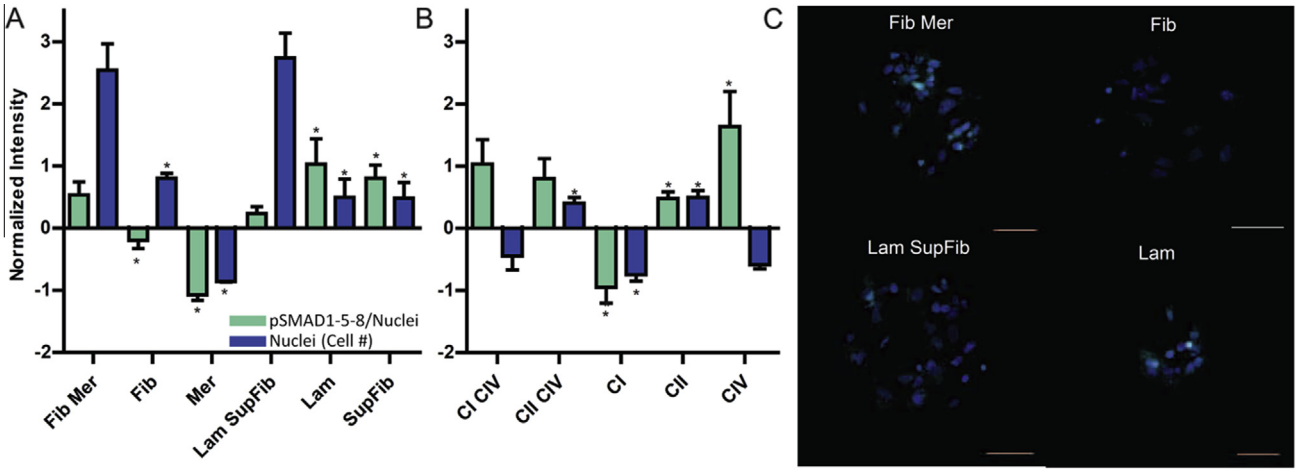

Fig. 6. Quantification of phosphorylated SMAD 1/5/8 within the ECM microarray platform. Immunostaining was performed to evaluate phosphorylation of SMAD 1/5/8 at day 2 of treatment with hepatic (BMP4/bFGF) inducing conditions. (A) Nuclei intensity (cell number) (blue bars) and pSMAD 1/5/8 intensity normalized by nuclei intensity (green bars) are illustrated for combinations containing fibronectin, merosin, laminin, and superfibronectin. * = $p < 0.05$ (Student's *t*-test), compared to fibronectin + merosin condition. (B) Select combinations and single components of collagen I, collagen II, and collagen IV. * = $p < 0.05$ (Student's *t*-test), compared to collagen I + collagen IV condition. (C) Representative ECM islands at day 3 post-induction towards hepatic lineage. Scale bars = 50 μm.

hypothesized that ECM can act as a modulator of signals generated in response to soluble factors, including the activation of SMAD1, SMAD5, and SMAD8 downstream of BMP4 signaling during hepatic differentiation. In addition, previous studies have observed an increase in histone H3 acetylation (K9 and K14) associated with the AFP promoter, and that blocking these modifications impaired development of the liver bud [15]. Thus, we explored the potential of our microarray platform to examine the effects of ECM on these intracellular events associated with hepatic differentiation.

To investigate the effects of ECM composition on SMAD activation, we utilized the 31 combination ECM array, and performed immunostaining of adherent cells to detect phosphorylated (p) SMAD1/5/8 following 48 h of treatment with BMP4 and bFGF (hepatic-inducing conditions, as employed above). Consistent with the observed impact on induction of AFP expression (Fig. 4A), the intensity of pSMAD1/5/8 expressed by cells bound to the fibronectin + merosin domain was significantly higher compared to cells present on the individual component spots (Fig. 6A and C). This result suggests that the positive effect of this ECM combination on hepatic lineage differentiation is at least correlated with, and may be mediated by SMAD signaling in response to BMP4 stimulation. In contrast, cells bound to individual laminin and superfibronectin domains exhibited elevated levels of pSMAD1/5/8 relative to the signaling present in cells bound to the combination of these ECM components (Fig. 6A and C). In addition, hepatic differentiation in the presence of various collagen combinations led to a range of SMAD activation profiles (Fig. 6B). Specifically, the intensity of pSMAD1/5/8 was elevated in cells on collagen IV-containing domains, either alone or in combination with collagen I or II. In comparison, adhesion to collagen I appeared to have a negative impact on SMAD 1/5/8 phosphorylation.

In addition to the SMAD pathway, we further evaluated overall histone H3 (K9 and K14) acetylation as surrogate readouts of epigenetic regulation within distinct ECM microenvironments. Employing the 31 combination ECM array as above, we performed immunostaining for H3K9ac and H3K14ac prior to and 48 h following induction of hepatic differentiation. Similar to the effects on SMAD activation, combinatorial ECM compositions influenced H3 acetylation (Supplemental Fig. 6). In particular, fibronectin + merosin exhibited increased H3K14 acetylation compared to fibronectin or merosin alone, which correlates well with the effects of ECM on SMAD 1/5/8 phosphorylation and the degree of hepatic differentiation as measured by AFP expression. Collectively, these studies demonstrate the utility of the ECM microarray platform for analyzing the effects of ECM binding on signaling pathway activation and epigenetic modifications, and the potential for correlating these

observations with differentiation outcomes across a panel of conditions and time points.

4. Discussion

In order to deconstruct the complex microenvironmental signaling mechanisms that regulate stem and progenitor fate decisions, higher throughput methods that enable the systematic analysis of combinations of signals are needed. Here, we utilized an ECM microarray platform to examine the role of cell-ECM interactions in endoderm differentiation. Previous efforts have utilized ECM microarrays for analyzing adhesion and differentiation within various cellular contexts. Building on these efforts, our studies represent a significant advancement of the ECM microarray approach in several ways. First, previous work incorporating large-scale combinatorial arrays (>740 distinct combinations of ECM proteins) has been focused on short-term readouts of cell function such as cell adhesion [5]. Here, we demonstrate the integration of such large-scale arrays with cell differentiation measurements. We further highlight the modularity of the microarray approach through the subsequent implementation of focused arrays consisting of subsets of combinations identified within the large-scale format. In addition, previous studies utilizing cell microarray systems to investigate cell differentiation have primarily focused on phenotypic markers [4,30,31]. In our studies here, we have expanded on this assessment of cell phenotypic markers, and additionally demonstrate the capability of an ECM microarray approach to enable investigations into cell signaling pathways that underlie cell differentiation processes.

Overall, our results illustrate how cell-ECM interactions evolve during endoderm differentiation to the hepatic or pancreatic lineages. One of the compelling results from these experiments is that upon differentiation induction within the array format, the ECM components that support significant adherent cell numbers rapidly change, and distinct profiles are observed following treatment with either hepatic or pancreatic inducing soluble factors. Several mechanisms may be contributing to the changes observed in these evolving profiles, including potential distinct effects of ECM and soluble factor combinations on cell survival, adhesion, and proliferation. By analyzing the activation of caspase-3, our results demonstrate that ECM can influence the degree of apoptosis (Supplemental Fig. 3) triggered during differentiation. These data suggest that following differentiation induction, alterations in ECM-derived survival signals occur, which at least partially contributes to the shifts in cell numbers detected within the array domains. It is likely that changes in ECM adhesion receptors, such as integrins, may also lead to direct cell detachment from the two-dimensional array surface. Although our findings suggest that the adhesion profiles of hepatic cells differentiated within the array or off-array are highly correlated (Fig. 4D), adhesion receptor expression analysis during differentiation would provide additional insight. Also, future studies incorporating time-lapse imaging, as well as the direct assessment of cell proliferation (e.g. quantification of BrDU incorporation) would aid the further decoupling of the effects of ECM on differentiating cell survival, adhesion, and proliferation.

Despite the increasingly recognized importance of ECM within stem and progenitor cell microenvironments [32], less is known regarding the temporal and spatial dynamics of cell-ECM interactions during the development of endoderm tissues. In lung and intestine, dynamic remodeling of ECM has been demonstrated to be critical in normal tissue development as well as the progression of certain diseases [33]. For liver, distinct developmental stages have been shown to exhibit distinct spatial patterns of integrin receptor expression [34]. Based on the evolving cell adhesion profiles we observed in our studies, we have hypothesized that there are dynamic alterations in the responses of cells to different ECM combinations during endoderm differentiation. Such alterations are consistent with findings in many developmental contexts in which response networks in cells change rapidly after a step in differentiation. For example, for pancreatic specification of endoderm, it has previously been demonstrated that BMP signaling is initially inhibitory, but then becomes an induction stimulus at a later developmental stage [35]. Towards the optimization of stem cell differentiation, it may be beneficial to tailor ECM substrates independently for each stage of differentiation, or alternatively identify a single ECM combination that could support many sequential stages. Thus, building on our results demonstrated here, we anticipate that high-throughput approaches, such as the ECM microarray platform, would enable the systematic assessment of cell-ECM dynamics and support the optimization of directed differentiation protocols.

ECM effects on the degree of differentiation were determined via the expression of hepatic (AFP) and pancreatic (Pdx1) markers in the array 3 days after induction (Fig. 3). Interestingly, differentiation towards the hepatic fate appears to be closely correlated with cell number (Fig. 3A). For pancreatic fate, the relationship is more complex, as the data illustrate that some ECM compositions support significant cell numbers and Pdx1 expression, while others exclusively support either increased relative Pdx1 expression or cell number (Fig. 3B). In comparing the ECM combinations that optimally support hepatic or pancreatic differentiation, a select few appear to support both lineages. In particular, the following two combinations consisting of forms of fibronectin and laminin exhibit this dually-supportive effect: fibronectin + merosin (laminin $\alpha 2$), and superfibronectin + laminin $\alpha 1$. Superfibronectin, which is a multimeric form of fibronectin, generally exhibits enhanced cell adhesive properties [36], and the effects of this molecule on hepatic and pancreatic differentiation have not previously been reported. Previous work analyzing fibronectin expression in mouse embryos has demonstrated that fibronectin is non-uniformly distributed during endoderm differentiation, and that a reduction in fibronectin content is involved in the development of the foregut region [37], which is the precursor region for liver and ventral pancreas. In addition, studies utilizing both mouse ES-derived cells and an *in vivo* zebrafish model, have suggested that fibronectin production by endoderm cells is critical for the differentiation of adjacent mesoderm [38]. Collectively, these *in vivo* findings together with our array results suggest that future studies systematically exploring the differential effects of fibronectin, including various forms such as superfibronectin, at more highly refined stages of endoderm differentiation are required.

In addition to the identification of the fibronectin and merosin condition, one of the most unexpected results from these experiments was the presence of collagen II in a number of combinations that supported hepatic differentiation, as collagen II is most commonly associated with cartilage differentiation [39]. Future experiments will be required to explore the potential physiologic relevance of collagen II effects on endoderm differentiation, however, several studies have identified collagen II expression in embryonic epithelial tissues [40–42]. Furthermore, in subsequent investigations it will be important to expand the analyses of ECM effects to include phenotypic markers for alternative lineages derived from endoderm not explored here, such as lung and thyroid. Together with the assessment of hepatic and pancreatic markers at the single cell level, such analyses of alternative lineages would provide additional information regarding the specificity of ECM conditions for directing distinct fates.

We further utilized the ECM microarray platform to investigate the activation of signaling pathways that may participate in the mechanisms of ECM-mediated modulation of hepatic lineage differentiation. Our results demonstrate differential SMAD1/5/8

signaling activation in different ECM compositions, which is suggestive of a potential synergistic interaction between ECM and BMP4, and warrants future investigation. Cooperation between ECM components and BMP4 has been previously been reported in the context of biliary differentiation of hepatoblasts within the developing liver [43]. In addition to SMAD signaling activation, we also explored potential effects of ECM on overall H3 histone acetylation. Future efforts will be aimed at analyzing the acetylation of histones associated with specific loci, such as the AFP promoter, towards determining the potential effects of ECM on these individual genes. Notably, the *in vivo* deletion of SMAD4, which cooperates with SMAD1/5/8 in BMP signaling, results in the loss of the acetyltransferase P300 at liver gene elements and a decrease in H3 acetylation [15]. Consequently, future efforts using scaled-up versions of the relevant ECM conditions identified here could be applied towards the examination of ECM composition as a potential modifying signal at the intersection of BMP signaling and epigenetic modifications such as histone acetylation.

In addition to mechanistic studies into ECM signaling effects, we anticipate that both the ECM microarray approach and findings reported here could aid in facilitating several processes related to cell sourcing and regenerative medicine applications. First, the identification of ECM conditions that most effectively support cell adhesion at distinct stages of differentiation could mitigate the common difficulties of enriching and replating cells after the initiation of the differentiation processes. Specifically, at each stage, the ECM microarray platform could be applied towards the systematic optimization of cell adhesion while additionally tailoring the differentiation towards downstream lineages. Interestingly, one of the ECM combinations highlighted in our results, fibronectin + merosin, exhibited the capacity to support DE cell adhesion, as well as supported both hepatic and pancreatic differentiation when cultured in corresponding hepatic and pancreatic induction mediums. Treatment of cell culture substrates with fibronectin + merosin, or similar ECM conditions, could serve a very practical purpose of generating robust endoderm cell adhesion for scaled-up liver or pancreas differentiation protocols, or also could be utilized as a substrate for future studies investigating combinatorial soluble or genetic factors regulating the liver and pancreas fate switch.

5. Conclusions

This report describes the systematic assessment of cell-ECM interactions during DE specification through the implementation of an ECM microarray approach that enables unbiased and high-throughput analysis. Large-scale arrays were complemented with smaller focused arrays consisting of subsets of relevant combinatorial ECM conditions. Utilizing this strategy, we demonstrate that ECM composition can influence differentiation trajectory, and for liver specification, ECM plays a modulatory role in signaling pathway activation and epigenetic alterations associated with effective differentiation. Overall, our studies highlight the capabilities of this platform for examining cell-ECM effects at a scale that more closely represents the complexity of ECM compositions *in vivo*. Consequently, this approach could be applied towards the study of cell fate decisions and signaling mechanisms within a broad number of tissue development and stem cell differentiation contexts.

Disclosures

The authors report no conflicts of interest.

Acknowledgments

The authors acknowledge D. Melton's laboratory (Harvard) for providing mouse embryonic stem cell lines, and S. Morrison's lab (UTSW) for sox17-GFP mouse embryonic stem cells. We further acknowledge the Koch Institute Swanson Biotechnology Center Core Facilities for technical support, specifically with tissue sectioning and flow cytometric cell sorting. This work has been funded in part by the Koch Institute Support Grant P30-CA14051 from the National Cancer Institute, and also supported in part by funding from the Harvard Stem Cell Institute. D.F.B.M. was supported in part by Fundação para a Ciência e Tecnologia, Portugal, through the MIT-Portugal Program, Bioengineering Systems Focus Area (Grant SFRH/BD/35357/2007). S.N.B. is an HHMI Investigator.

Appendix A. Supplementary data

Supplementary data associated with this article can be found, in the online version, at http://dx.doi.org/10.1016/j.actbio.2016.02.014.

References

[1] Y. Soen, A. Mori, T.D. Palmer, P.O. Brown, Exploring the regulation of human neural precursor cell differentiation using arrays of signaling microenvironments, Mol. Syst. Biol. 2 (2006) 37.
[2] M.A. LaBarge, C.M. Nelson, R. Villadsen, A. Fridriksdottir, J.R. Ruth, M.R. Stampfer, O.W. Petersen, M.J. Bissell, Human mammary progenitor cell fate decisions are products of interactions with combinatorial microenvironments, Integr. Biol. (Camb.) 1 (2009) 70–79.
[3] Y. Mei, K. Saha, S.R. Bogatyrev, J. Yang, A.L. Hook, Z.I. Kalcioglu, S.W. Cho, M. Mitalipova, N. Pyzocha, F. Rojas, K.J. Van Vliet, M.C. Davies, M.R. Alexander, R. Langer, R. Jaenisch, D.G. Anderson, Combinatorial development of biomaterials for clonal growth of human pluripotent stem cells, Nat. Mater. 9 (2010) 768–778.
[4] C.J. Flaim, S. Chien, S.N. Bhatia, An extracellular matrix microarray for probing cellular differentiation, Nat. Methods 2 (2005) 119–125.
[5] N.E. Reticker-Flynn, D.F. Malta, M.M. Winslow, J.M. Lamar, M.J. Xu, G.H. Underhill, R.O. Hynes, T.E. Jacks, S.N. Bhatia, A combinatorial extracellular matrix platform identifies cell-extracellular matrix interactions that correlate with metastasis, Nat. Commun. 3 (2012) 1122.
[6] J. Jung, M. Zheng, M. Goldfarb, K.S. Zaret, Initiation of mammalian liver development from endoderm by fibroblast growth factors, Science 284 (1999) 1998–2003.
[7] G. Deutsch, J. Jung, M. Zheng, J. Lora, K.S. Zaret, A bipotential precursor population for pancreas and liver within the embryonic endoderm, Development 128 (2001) 871–881.
[8] J.M. Rossi, N.R. Dunn, B.L. Hogan, K.S. Zaret, Distinct mesodermal signals, including BMPs from the septum transversum mesenchyme, are required in combination for hepatogenesis from the endoderm, Genes Dev. 15 (2001) 1998–2009.
[9] D. Stafford, V.E. Prince, Retinoic acid signaling is required for a critical early step in zebrafish pancreatic development, Curr. Biol. 12 (2002) 1215–1220.
[10] N. Tiso, A. Filippi, S. Pauls, M. Bortolussi, F. Argenton, BMP signalling regulates anteroposterior endoderm patterning in zebrafish, Mech. Dev. 118 (2002) 29–37.
[11] S. Roy, T. Qiao, C. Wolff, P.W. Ingham, Hedgehog signaling pathway is essential for pancreas specification in the zebrafish embryo, Curr. Biol. 11 (2001) 1358–1363.
[12] P.J. dilorio, J.B. Moss, J.L. Sbrogna, R.O. Karlstrom, L.G. Moss, Sonic hedgehog is required early in pancreatic islet development, Dev. Biol. 244 (2002) 75–84.
[13] A. Bhushan, N. Itoh, S. Kato, J.P. Thiery, P. Czernichow, S. Bellusci, R. Scharfmann, Fgf10 is essential for maintaining the proliferative capacity of epithelial progenitor cells during early pancreatic organogenesis, Development 128 (2001) 5109–5117.
[14] A. Hart, S. Papadopoulou, H. Edlund, Fgf10 maintains notch activation, stimulates proliferation, and blocks differentiation of pancreatic epithelial cells, Dev. Dyn. 228 (2003) 185–193.
[15] C.R. Xu, P.A. Cole, D.J. Meyers, J. Kormish, S. Dent, K.S. Zaret, Chromatin "prepattern" and histone modifiers in a fate choice for liver and pancreas, Science 332 (2011) 963–966.
[16] E. Forsberg, A. Lindblom, M. Paulsson, S. Johansson, Laminin isoforms promote attachment of hepatocytes via different integrins, Exp. Cell Res. 215 (1994) 33–39.
[17] M. Dziadek, Role of laminin-nidogen complexes in basement membrane formation during embryonic development, Experientia 51 (1995) 901–913.
[18] C.A. Crisera, A.S. Kadison, G.D. Breslow, T.S. Maldonado, M.T. Longaker, G.K. Gittes, Expression and role of laminin-1 in mouse pancreatic organogenesis, Diabetes 49 (2000) 936–944.
[19] Y. Higuchi, N. Shiraki, K. Yamane, Z. Qin, K. Mochitate, K. Araki, T. Senokuchi, K. Yamagata, M. Hara, K. Kume, S. Kume, Synthesized basement membranes direct the differentiation of mouse embryonic stem cells into pancreatic lineages, J. Cell Sci. 123 (2010) 2733–2742.

[20] N. Shiraki, T. Yamazoe, Z. Qin, K. Ohgomori, K. Mochitate, K. Kume, S. Kume, Efficient differentiation of embryonic stem cells into hepatic cells in vitro using a feeder-free basement membrane substratum, PLoS One 6 (2011) e24228.
[21] T. Yamazoe, N. Shiraki, M. Toyoda, N. Kiyokawa, H. Okita, Y. Miyagawa, H. Akutsu, A. Umezawa, Y. Sasaki, K. Kume, S. Kume, A synthetic nanofibrillar matrix promotes in vitro hepatic differentiation of embryonic stem cells and induced pluripotent stem cells, J. Cell Sci. 126 (2013) 5391–5399.
[22] C.J. Flaim, S. Chien, S.N. Bhatia, An extracellular matrix microarray for probing cellular differentiation, Nat. Methods 2 (2005) 119–125.
[23] A.E.J.T. Carpenter, M.R. Lamprecht, C. Clarke, I.H. Kang, O. Friman, D.A. Guertin, J.H. Chang, R.A. Lindquist, J. Moffat, P. Golland, D.M. Sabatini, Cell profiler: image analysis software for identifying and quantifying cell phenotypes, Genome Biol. 7 (2006) R100.
[24] I. Kim, T.L. Saunders, S.J. Morrison, Sox17 dependence distinguishes the transcriptional regulation of fetal from adult hematopoietic stem cells, Cell 130 (2007) 470–483.
[25] K.K. Niakan, H. Ji, R. Maehr, S.A. Vokes, K.T. Rodolfa, R.I. Sherwood, M. Yamaki, J.T. Dimos, A.E. Chen, D.A. Melton, A.P. McMahon, K. Eggan, Sox17 promotes differentiation in mouse embryonic stem cells by directly regulating extraembryonic gene expression and indirectly antagonizing self-renewal, Genes Dev. 24 (2010) 312–326.
[26] L.B. Corson, Y. Yamanaka, K.M. Lai, J. Rossant, Spatial and temporal patterns of ERK signaling during mouse embryogenesis, Development 130 (2003) 4527–4537.
[27] A. Calmont, E. Wandzioch, K.D. Tremblay, G. Minowada, K.H. Kaestner, G.R. Martin, K.S. Zaret, An FGF response pathway that mediates hepatic gene induction in embryonic endoderm cells, Dev. Cell 11 (2006) 339–348.
[28] M. Borowiak, R. Maehr, S. Chen, A.E. Chen, W. Tang, J.L. Fox, S.L. Schreiber, D.A. Melton, Small molecules efficiently direct endodermal differentiation of mouse and human embryonic stem cells, Cell Stem Cell 4 (2009) 348–358.
[29] V. Allamand, P. Guicheney, Merosin-deficient congenital muscular dystrophy, autosomal recessive (MDC1A, MIM#156225, LAMA2 gene coding for alpha2 chain of laminin), Eur. J. Hum. Genet.: EJHG 10 (2002) 91–94.
[30] D.A. Brafman, S. de Minicis, E. Seki, K.D. Shah, D. Teng, D. Brenner, K. Willert, S. Chien, Investigating the role of the extracellular environment in modulating hepatic stellate cell biology with arrayed combinatorial microenvironments, Integr. Biol. (Camb.) 1 (2009) 513–524.
[31] D.A. Brafman, K.D. Shah, T. Fellner, S. Chien, K. Willert, Defining long-term maintenance conditions of human embryonic stem cells with arrayed cellular microenvironment technology, Stem Cells Dev. 18 (2009) 1141–1154.
[32] F. Gattazzo, A. Urciuolo, P. Bonaldo, Extracellular matrix: a dynamic microenvironment for stem cell niche, Biochim. Biophys. Acta 1840 (2014) 2506–2519.
[33] C. Bonnans, J. Chou, Z. Werb, Remodelling the extracellular matrix in development and disease, Nat. Rev. Mol. Cell Biol. 15 (2014) 786–801.
[34] N. Shiojiri, Y. Sugiyama, Immunolocalization of extracellular matrix components and integrins during mouse liver development, Hepatology 40 (2004) 346–355.
[35] E. Wandzioch, K.S. Zaret, Dynamic signaling network for the specification of embryonic pancreas and liver progenitors, Science 324 (2009) 1707–1710.
[36] A. Morla, Z. Zhang, E. Ruoslahti, Superfibronectin is a functionally distinct form of fibronectin, Nature 367 (1994) 193–196.
[37] SN Villegas, M Rothova, ME Barrios-Llerena, M Pulina, AK Hadjantonakis, T Le Bihan, S Astrof, JM Brickman, PI3K/Akt1 signalling specifies foregut precursors by generating regionalized extra-cellular matrix, in: eLife 2 (2013) e00806.
[38] P. Cheng, P. Andersen, D. Hassel, B.L. Kaynak, P. Limphong, L. Juergensen, C. Kwon, D. Srivastava, Fibronectin mediates mesendodermal cell fate decisions, Development 140 (2013) 2587–2596.
[39] E.J. Miller, V.J. Matukas, Chick cartilage collagen: a new type of alpha 1 chain not present in bone or skin of the species, Proc. Natl. Acad. Sci. USA 64 (1969) 1264–1268.
[40] R.A. Kosher, M. Solursh, Widespread distribution of type II collagen during embryonic chick development, Dev. Biol. 131 (1989) 558–566.
[41] V.C. Lui, L.J. Ng, J. Nicholls, P.P. Tam, K.S. Cheah, Tissue-specific and differential expression of alternatively spliced alpha 1(II) collagen mRNAs in early human embryos, Dev. Dyn. 203 (1995) 198–211.
[42] E. Kolpakova-Hart, C. Nicolae, J. Zhou, B.R. Olsen, Col2-Cre recombinase is co-expressed with endogenous type II collagen in embryonic renal epithelium and drives development of polycystic kidney disease following inactivation of ciliary genes, Matrix Biol.: J. Int. Soc. Matrix Biol. 27 (2008) 505–512.
[43] M. Yanai, N. Tatsumi, N. Hasunuma, K. Katsu, F. Endo, Y. Yokouchi, FGF signaling segregates biliary cell-lineage from chick hepatoblasts cooperatively with BMP4 and ECM components in vitro, Dev. Dyn. 237 (2008) 1268–1283.
[44] A.E. Carpenter, T.R. Jones, M.R. Lamprecht, C. Clarke, I.H. Kang, O. Friman, D.A. Guertin, J.H. Chang, R.A. Lindquist, J. Moffat, P. Golland, D.M. Sabatini, Cell profiler: image analysis software for identifying and quantifying cell phenotypes, Genome Biol. 7 (2006) R100.

Supplemental Data

Supplemental Figure 1: Enrichment of mouse ES-derived definitive endoderm cells

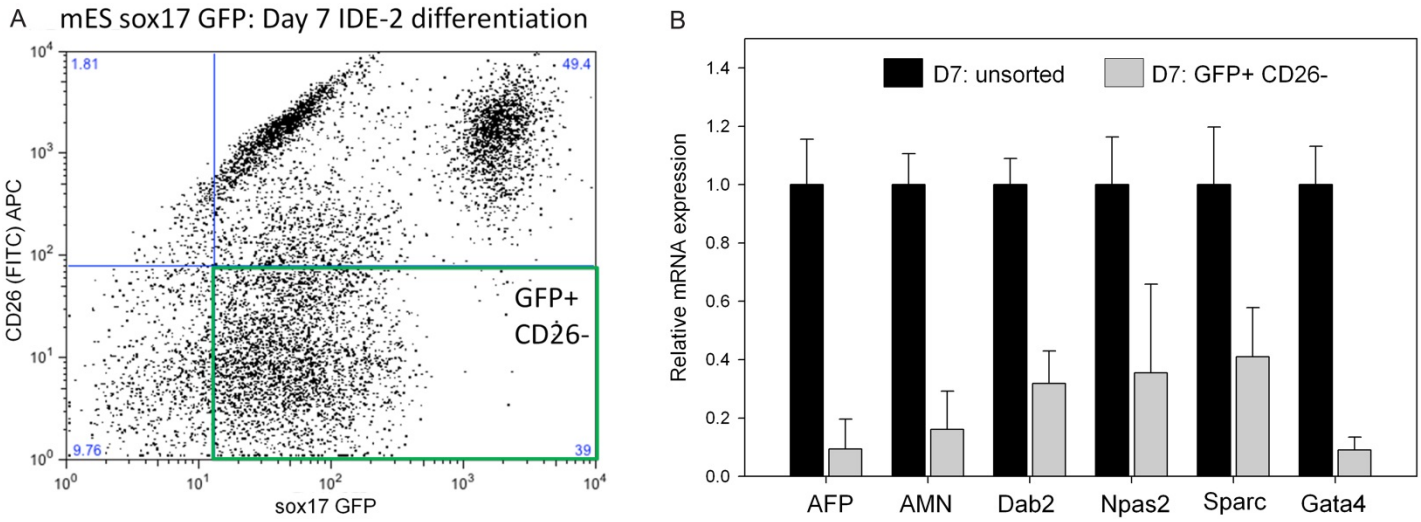

A) Representative flow cytometry scatter plot illustrating sox17 GFP and CD26 expression following 7 day differentiation of mouse embryonic stem cells in the presence of IDE-2. Approximately 39% of cells were GFP+ and CD26- definitive endoderm cells, and this population (green box) was isolated and seeded on ECM microarrays.

B) Real-time PCR-based mRNA expression analysis of a panel of 6 visceral endoderm genes. Sorting for GFP+ CD26- definitive endoderm cells at day 7 results in the reduction in expression for each of these genes, indicating that visceral endoderm cells are substantially removed during the sorting process.

Supplemental Figure 2: Assessment of endoderm phenotypic markers following ECM microarray adhesion

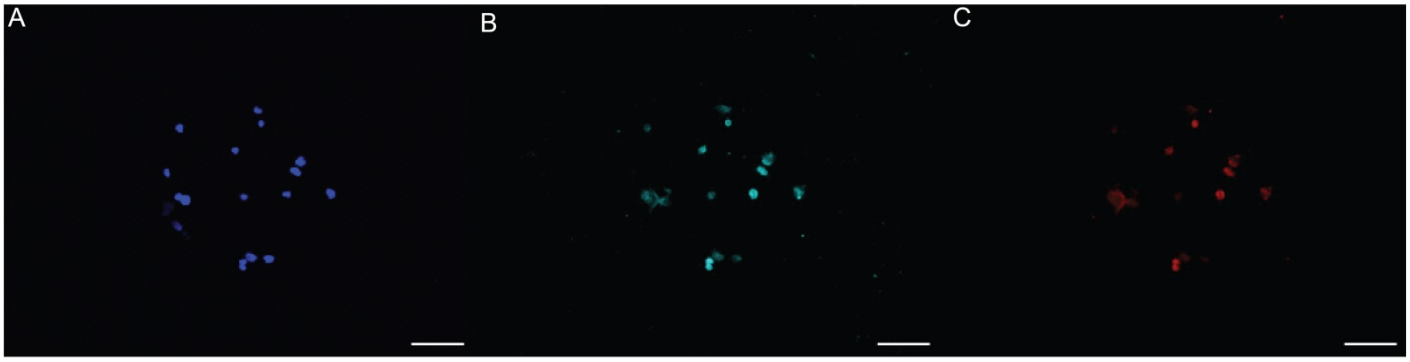

A-C) Representative images of immunofluorescence-based analysis of cell nuclei (A) and definitive endoderm markers Sox17 (B) and Foxa2 (C) 12 hours post-seeding on large scale (741 combination) ECM microarrays.

Supplemental Figure 3: Quantification of activated caspase-3 following hepatic or pancreatic induction

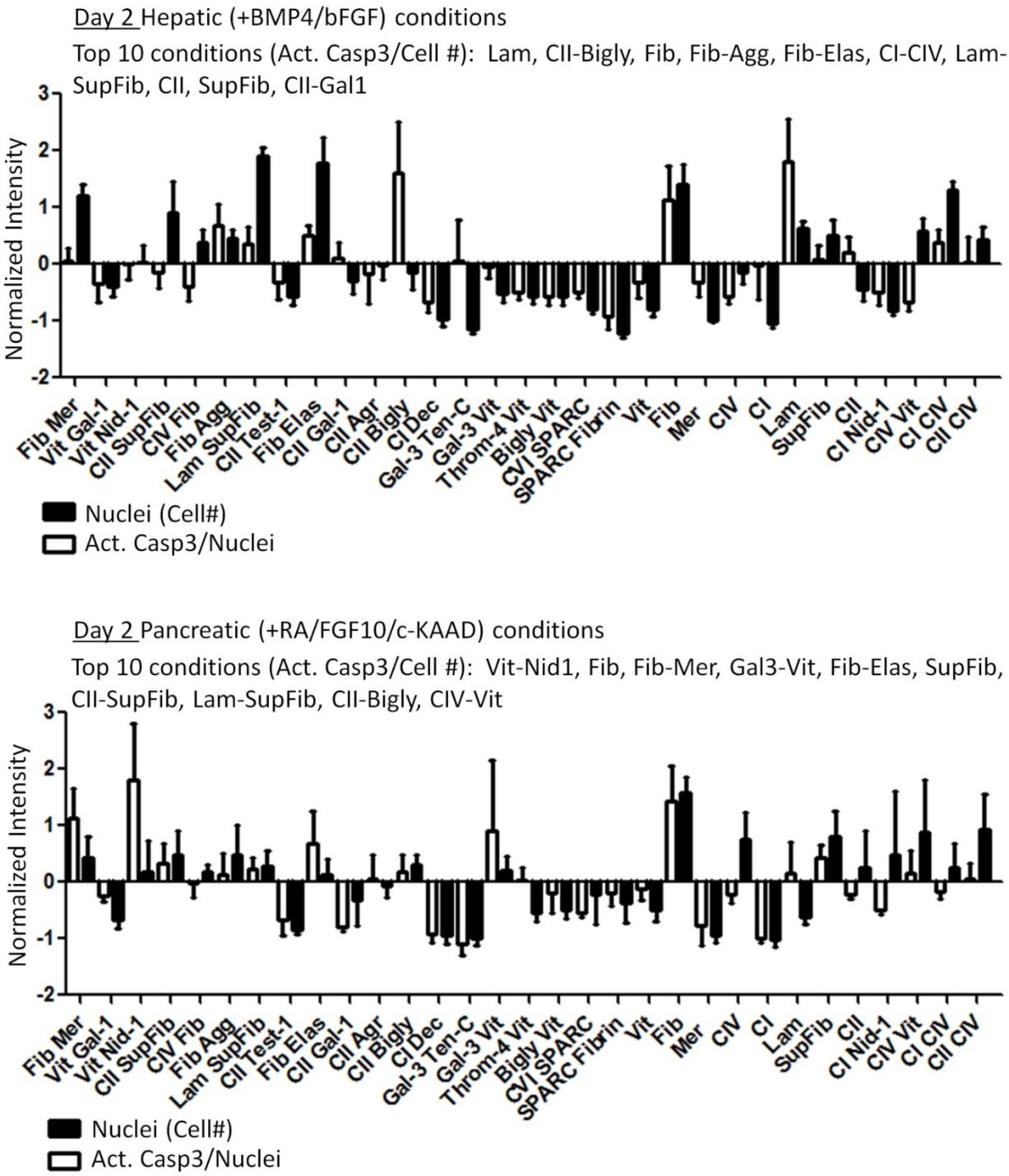

Nuclei intensity (cell number) (black bars) and activated caspase-3 immunostain intensity normalized by nuclei intensity (white bars) at day 2 following treatment with either hepatic or pancreatic inducing conditions. Among the ECM conditions that lead to the greatest activated caspase-3 per cell at day 2 (top 10 conditions from plots listed), select combinations are shared between hepatic and pancreatic conditions while several are unique to the respective treatment.

Supplemental Figure 4: Effects of ECM combinations on hepatic and pancreatic differentiation (31 ECM combination array)

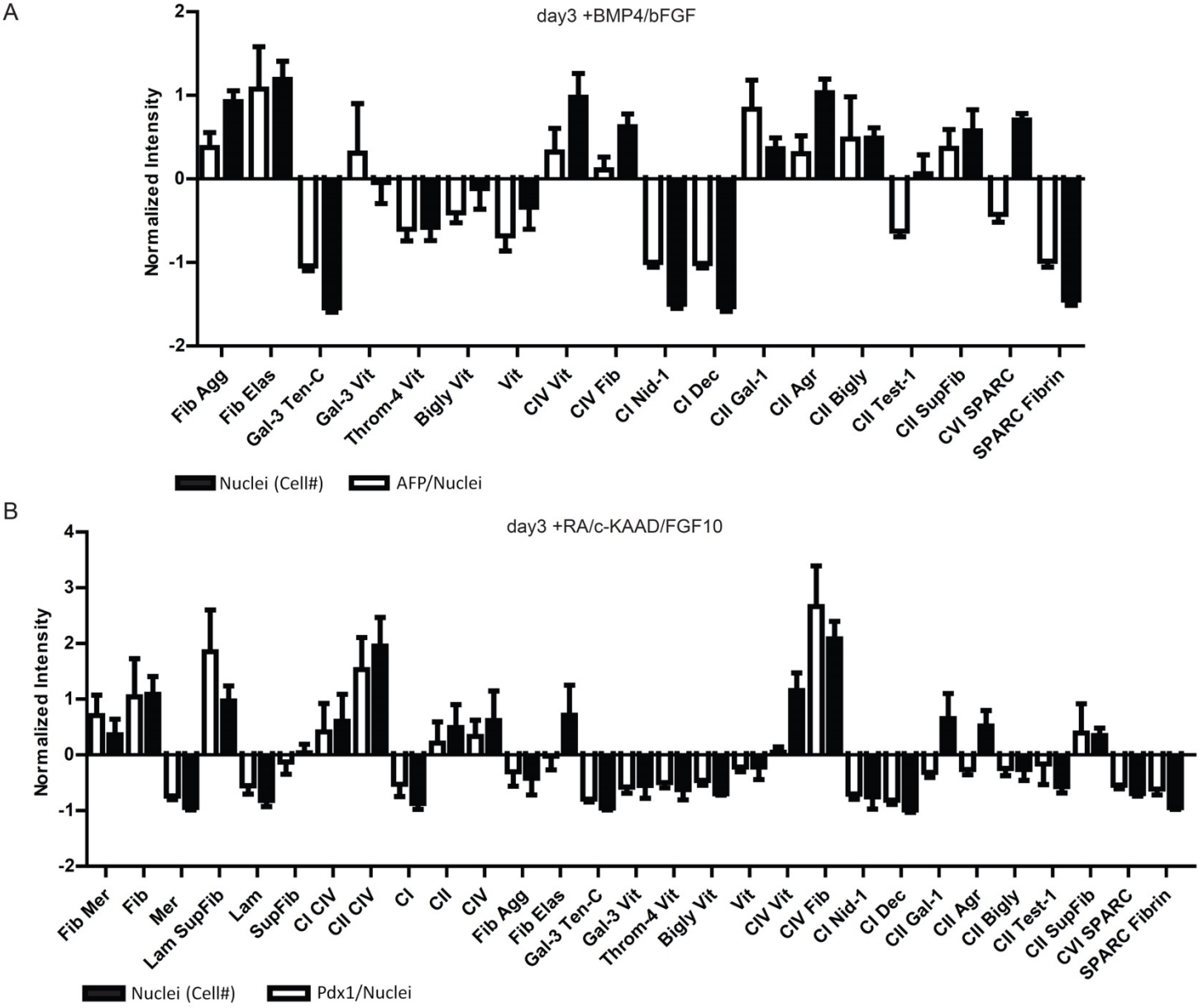

(A) AFP expression and cell number data from 31 ECM combination focused array, not included in Figure 4. Nuclei intensity (cell number) (black bars) and AFP intensity normalized by nuclei following 3 days of hepatic (BMP4/bFGF) induction conditions.

(B) Nuclei intensity (cell number) (black bars) and Pdx1 intensity normalized by nuclei 3 days following 3 days of pancreatic (RA/c-KAAD/FGF10) induction conditions.

Supplemental Figure 5: AFP and Pdx1 mRNA expression on Fibronectin + Merosin in multiwell plate

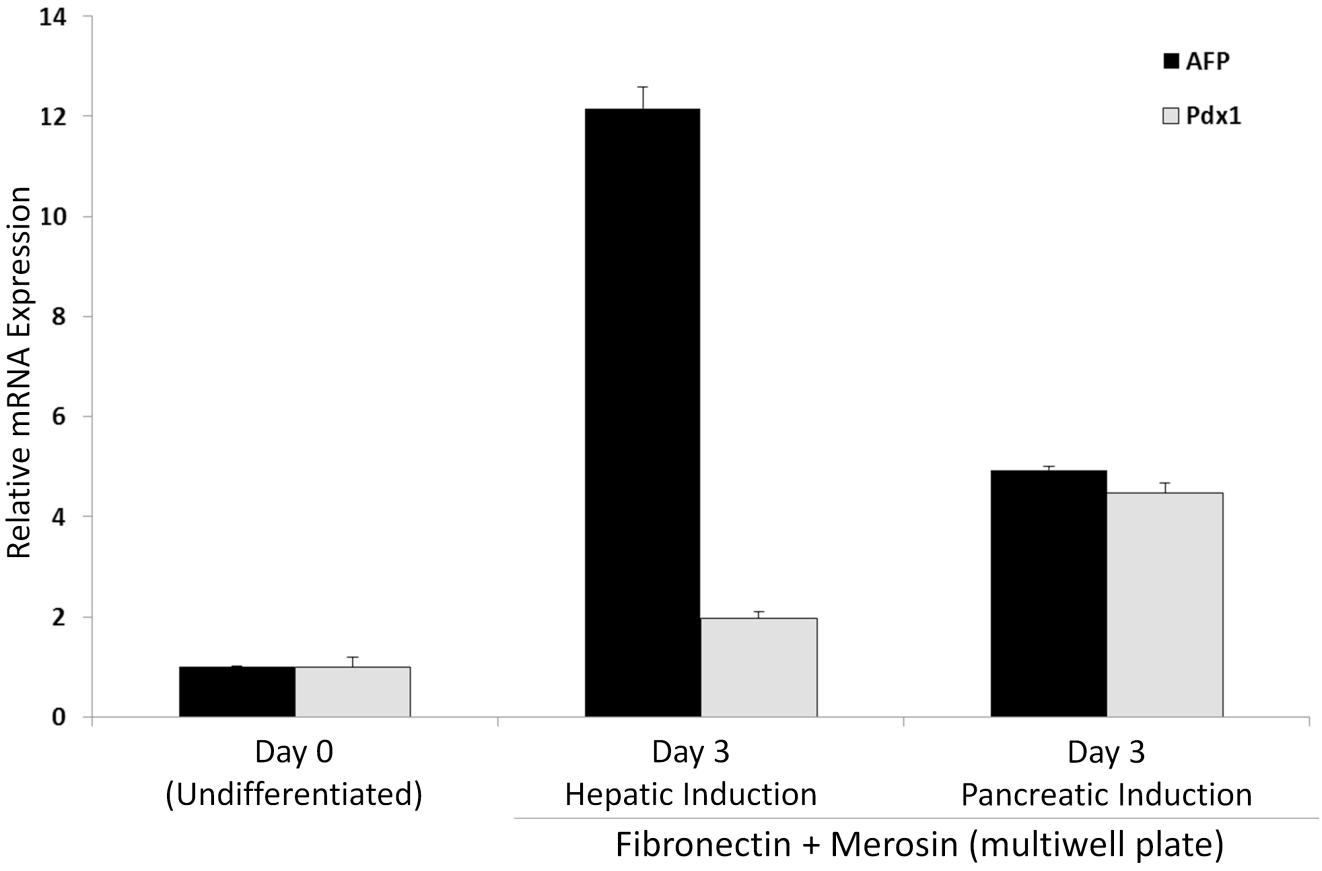

Real-time PCR-based mRNA expression analysis of AFP and Pdx1 genes for day 0 undifferentiated definitive endoderm cells (sorted GFP+ Cd26-) and cells following 3 days of differentiation in hepatic (+BMP4/bFGF) or pancreatic (+RA/FGF10/c-KAAD) conditions. Cells were seeded within wells of a 12-well plate that was previously treated for 1 hr with 100 μg/ml Fibronectin and 100 μg/ml Merosin.

Supplemental Figure 6: Analysis of cellular histone acetylation within ECM microarray

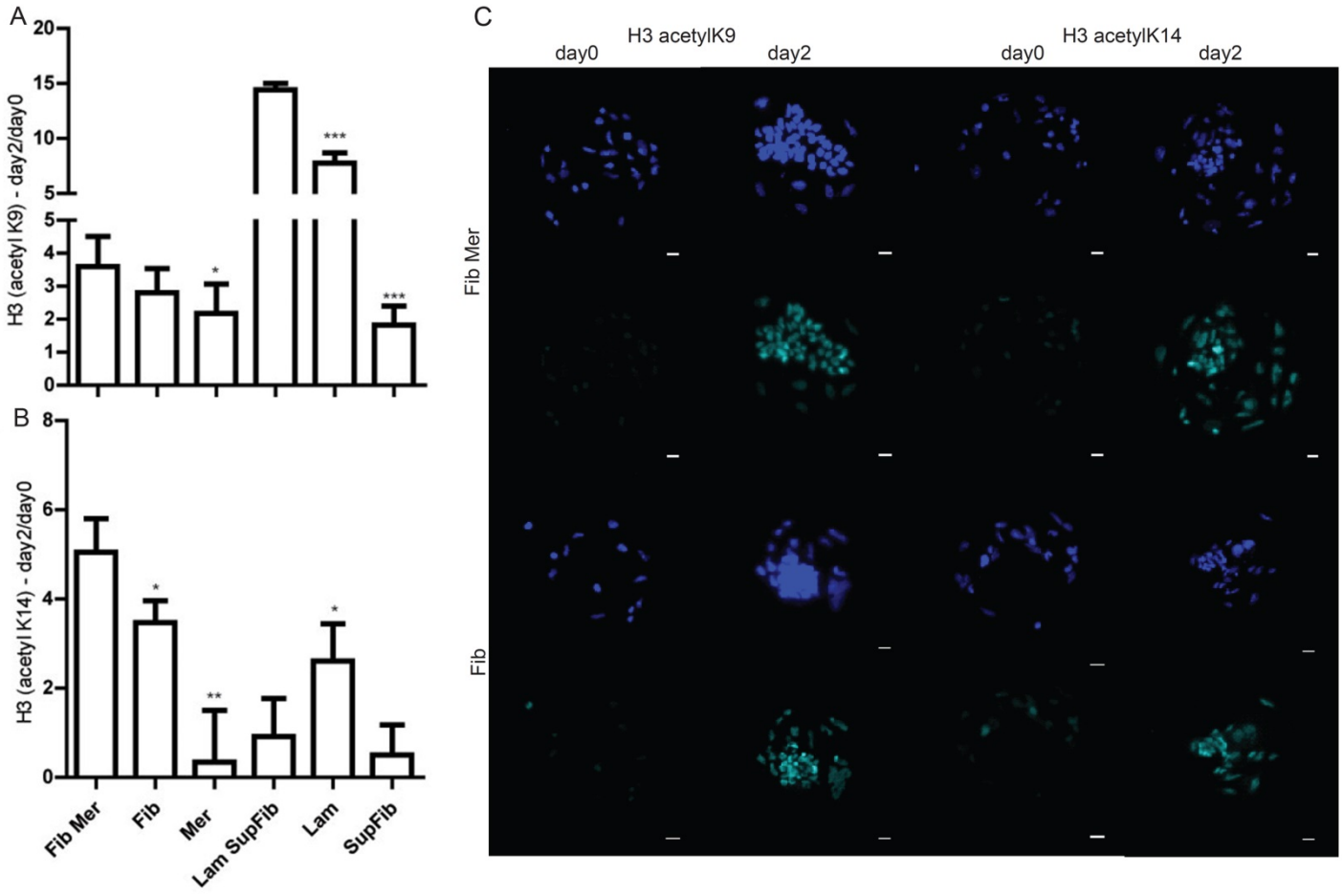

A-C) Immunostaining-based quantitative assessment of H3K9 and H3K14 acetylation within defined ECM conditions of ECM microarray at day 0 and day 2 of hepatic (BMP4/bFGF) induction conditions. Ratio of H3K9 (A) and H3K14 (B) acetylation at day 2 versus day 0for select ECM conditions. (C) Representative images of histone acetylation (green) and corresponding cell nuclei (blue) for fibronectin + merosin and fibronectin alone. Statistical significance was determined using Student's t-test between the single molecules and the corresponding combinations of two molecules. * = $p<0.05$, ** = $p<0.02$, *** = $p<0.01$.

Supplemental Methods

RNA isolation and qRT-PCR analysis

Cell lysates were collected in TRIzol solution (Life Technologies, 15596-026) from which RNA was isolated using phenol-chloroform extraction per the manufacturer's instructions. Samples were subsequently digested with DNAse (New England Biolabs, M0303S) at 37°C for 30 min and cleaned using an RNeasy Mini Kit (Qiagen, 74104) per the manufacturer's instructions. 0.5 μg of total RNA was used in 20 μl cDNA synthesis reactions utilizing the iScript™ cDNA synthesis kit (Bio-Rad, Hercules, CA) according to the manufacturer's protocol, and reactions performed in the absence of reverse-transcriptase enzyme were used as negative controls. cDNA products then served as templates in 25 μl PCR reactions with the iQ™ SYBR green supermix (Bio-Rad) and reactions were performed and analyzed using the MyiQ™ real-time PCR detection system (Bio-Rad). The cycling parameters were 95 °C for 3 min then 40 cycles of 95 °C for 10s and 60 °C for 45s. Primers were used at 100 nM and were purchased from Integrated DNA Technologies (Coralville, IA). Primer sequences are available upon request. HPRT mRNA expression was utilized as a normalization control.

Primer pairs

Gene Symbol	**GenBank Accession**	**Sequence (5'-to-3')**
AFP	NM_007423.4	Forward: TGA CAA CAA GGA GGA GTG CTT CCA Reverse: AAT GGT TGT TGC CTG GAG GTT TCG
AMN	NM_033603.3	Forward: ATT GTC TTC AAG CAG CAG CCT TCG Reverse: GTT AAC GAA GCA GCC GAA CTT GGT
Dab2	NM_023118	Forward: TGC CTT CCC GTC ATG TCT AAC GAA Reverse: CAC CTT TGA ACC TGG CCA ACA AGT
Npas2	NM_008719	Forward: TTG AAG TAC TTG GCA CCT CAG GCT Reverse: CGA CTT CCC TTT GCC AAA CTG CAT
Sparc	NM_009242	Forward: TGT TGG CCC GAG ACT TTG AGA AGA Reverse: ACC CAT CAA TAG GGT GCT GAT CCA
Gata4	NM_008092	Forward: AGGGTGAGCCTGTATGTAATGCCT Reverse: AGGACCTGCTGGCGTCTTAGATTT
Hprt1	NM_013556.2	Forward: GGAGTCCTGTTGATGTTGCCAGTA Reverse: GGGACGCAGCAACTGACATTTCTA